4th Specialty Conference on Coastal, Estuary and Offshore Engineering
4e Conférence spécialisée sur l'ingénierie côtière et en milieu maritime

Montréal, Québec
May 29 to June 1, 2013 / *29 mai au 1 juin 2013*

Tidal Analysis of Sea Reclamation Project in Dalian Laohutan Bay

Ke Wang[1], Xi Zhang[1], Z. Chen[2]

[1]State Key Laboratory of Structural Analysis for Industrial Equipment, Department of Engineering Mechanics, Dalian University of Technology, Dalian 116024, China

[2]Concordia University, 1455 de Maisonneuve W, Montreal, QCH3G 1M8, Canada

Abstract: A tidal analysis model, Mike 21 HD FM is utilized to simulate the flow field of Dalian Laohutan Bay during the sea reclamation project to assess the impacts of the project on flow fields and water quality. The good agreement between the predicted flow fields and the field measured data indicates the model is accurate. The validated model is applied to investigate the effect of the sea reclamation project in Dalian Laohutan Bay. A series of simulations are executed for the existing and planned topographies of bay according to the well-planned scenarios. Predicted flow fields and parameters including influx and discharge from different scenarios are compared to select the scenario that can achieve sound engineering design to reduce impact on water quality due to the sea reclamation project.

1. Introduction

Laohutan Bay is located on the south of Dalian city (at 121° 39′ E ~ 121° 40′ E，38°51′ N ~ 38° 53′ N) and near the west of Sanshan Island. Its geographical location is shown in Figure1.

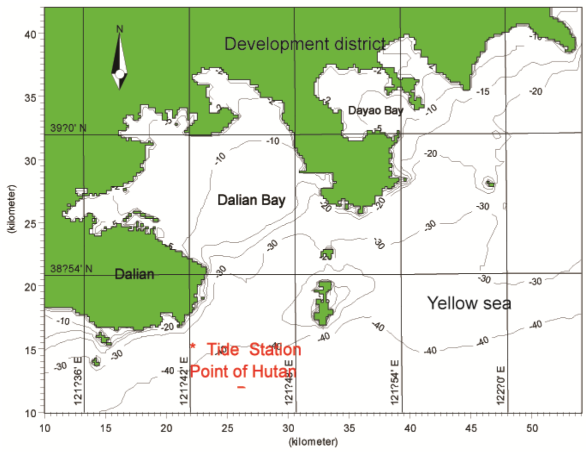

Figure 1: Geographical location of Laohutan Bay

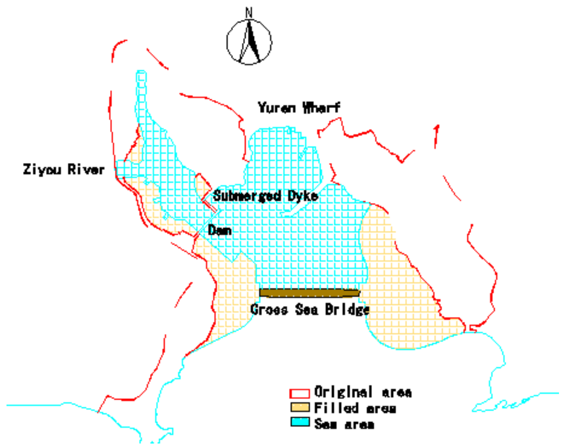

Figure 2: Calculation Scope of Laohutan Bay

The Dalian Laohutan Ocean Park, located in Dalian Laohutan Bay, has ranked one of the first national Five-A-Class scenic areas in Liaoning Province of north China. However, with the rapid tourism development, the Dalian Laohutan ocean park could not meet the increasing demands in such scale of zone area. In 2012, the sea reclamation project in Dalian Laohutan Bay has been launched by the Dalian government. The reclamation of the Laohutan Bay covers the North Great Bridge on the west and the Xiaoshicao area on the east. The total land reclamation area is 2.14 square kilometers, of which 1.01 square kilometers are sea field where the rest 0.376 square kilometers is the reclaiming land from the sea. The reclamation project of Figure 2 in Dalian Laohutan Bay includes three procedures: the building of coastal landscape along the bay; construction of cross-sea bridge (North Great Bridge); and sea reclamation (zone with yellow color). The land reclamation project is complicated and many environmental components should be considered such as wave propagation, tidal analysis, water exchange, mud or sand transportation, diffusion of contaminant and so on. Due to the land reclamation, the whole water capacity in the bay will be greatly decreased and thus the first and urgent task in this project is to find the solution of the water exchange problem especially within the inner field between the Ziyou River and the submerged dyke and the dam. Only from the viewpoint of physical process, a possible measure, adding openings and gates on the submerged dyke and dam, is suggested to solve the problem. The recommended scenario is to let more clean water run into the inner field of the bay and keep the water quality less contaminated.

This paper presents the results of tidal analysis to give a reasonable environmental evaluation about flow motion within the whole domain and water exchange on the cross-sections at interested zones. The results will give the opportunity to determine the effect of reclamation and to compare simultaneously the influx and discharge of tide accumulation under different cross-sections. The following sections includes: the mathematical model of the flow field changes inside the bay; the numerical procedure utilizing the HD FM mode of the MIKE 21 (2007) and the case studies; the velocity distribution of high tide at rising and falling time; the analysis of the maximum and the average flow velocities for different scenarios; the influx and discharge of tide accumulation on definite cross-sections; and finally conclusion and remarks.

2. Mathematical Model of the Tide

2.1 The governing equations

As for the near shore tide that the horizontal scale is bigger than the vertical one, the change of hydraulic parameters such as the water depth and the flow velocity is much smaller in the vertical direction than in the horizontal direction. Assuming the velocity in the direction of water depth is constant, it is feasible to integrate the three-dimensional (3D) Reynolds-averaged Navier-Stokes (RANS) equations for incompressible flow along the water depth to consider the flow as two dimensional (2D). Then, the governing equations for 2D shallow water flow based on the conservation of mass (continuity) and the momentum can be written.

Continuous equation:

[1] $$\frac{\partial h}{\partial t}+\frac{\partial h\bar{u}}{\partial x}+\frac{\partial h\bar{v}}{\partial y}=hS$$

The momentum equation in the x direction:

[2]
$$\frac{\partial h\bar{u}}{\partial t}+\frac{\partial h\bar{u}^{2}}{\partial x}+\frac{\partial h\overline{uv}}{\partial y}=f\bar{v}h-gh\frac{\partial h}{\partial x}-\frac{h}{r_0}\frac{\partial p_a}{\partial x}-\frac{gh^2}{2r_0}\frac{\partial r}{\partial x}+ \frac{t_{sx}}{r_0}-\frac{t_{bx}}{r_0}-\frac{1}{r_0}\left(\frac{\partial s_{xx}}{\partial x}+\frac{\partial s_{xy}}{\partial y}\right)+\frac{\partial}{\partial x}(hT_{xx})+\frac{\partial}{\partial y}(hT_{xy})+hu_sS$$

The momentum equation in the y direction:

[3]
$$\frac{\partial h\bar{v}}{\partial t}+\frac{\partial h\overline{uv}}{\partial x}+\frac{\partial h\bar{v}^{2}}{\partial y}=-f\bar{u}h-gh\frac{\partial h}{\partial y}-\frac{h}{r_0}\frac{\partial r_a}{\partial y}-\frac{gh^2}{2r_0}\frac{\partial r}{\partial y}+\frac{t_{xy}}{r_0}- \frac{t_{by}}{r_0}-\frac{1}{r}\left(\frac{\partial s_{yx}}{\partial x}+\frac{\partial s_{yy}}{\partial y}\right)+\frac{\partial}{\partial x}(hT_{xy})+\frac{\partial}{\partial y}(hT_{yy})+hv_sS$$

where $h\bar{u}=\int_{-d}^{h}udz$; $h\bar{v}=\int_{-d}^{h}vdz$.

T_{ij} denotes variables such as friction and eddy viscosity resistance. Its components are defined as follows:

[4]
$$\begin{cases} T_{xx}=2A\dfrac{\partial\bar{u}}{\partial x} \\ T_{xy}=A\left(\dfrac{\partial\bar{u}}{\partial y}+\dfrac{\partial\bar{v}}{\partial x}\right) \\ T_{yy}=2A\dfrac{\partial\bar{v}}{\partial y} \end{cases}$$

2.2 Numerical Method and Boundary Conditions

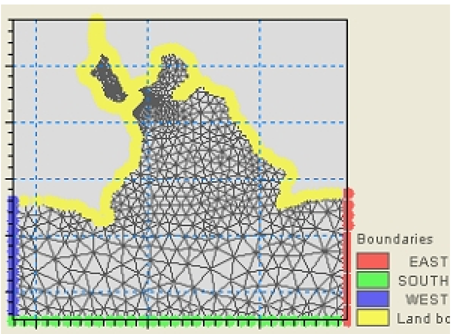

Figure 3 Mesh and boundary conditions

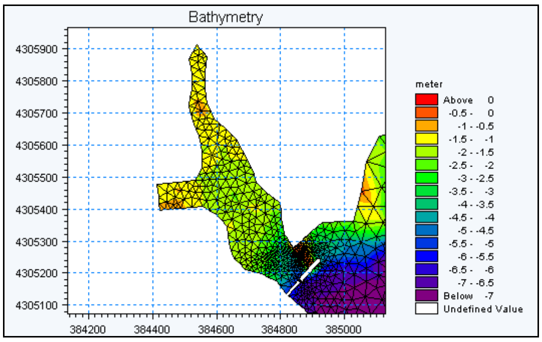

Figure 4 Mesh of zone 1

The finite volume method (FVM) is utilized in the numerical calculation to solve the governing equations, and the low order Eulerian method is adopted in time integration. The planning of Laohutan reclamation project is shown in Figure 2. The whole fluid domain is divided into four zones: the area between Ziyou River and submerged dyke and dam (zone 1); the area inside Yuren Wharf (zone 2); the area between North Great Bridge and dam (zone 3); and the area outside North Great Bridge (zone 4). Triangular meshing grid with varying cell distribution is adopted in the four zones. The maximum grid cell areas in each of the zones are 100 m^2, 500 m^2, 2000 m^2 and 10000 m^2, respectively. The minimum grid cell size of

2 m^2 is used for the gates on the dam to resolve the large velocity gradient. The mesh sizes mentioned above allows maintaining the corresponding Courant number (C) less than 0.8 at any adaptive time step for numerical stability (i.e., the smallest time step size of 0.01 seconds; the largest time step size of 120 seconds). The extent of the numerical domain representing the physical boundary is 3.0 km by 2.7 km, and the numerical grid is consisted of 1552 nodes and 2666 elements. The chosen extent of the numerical domain and grid dimension is sufficient to predict the whole flow fields in the entire area of the reclamation project.

2.3 Model Validation

After the establishment of the model, firstly, the field investigation to monitor the flow fields was conducted to determine the boundary conditions. According to the tidal requirements of the Laohutan Bay project, temporary observation stations were built near the project site (stations A, B, C, D and E in Figure 5), and the time of tides and flow spans were monitored from 16 o'clock on April 16th, 2010 to 16 o'clock on April 22nd, 2010. Three open boundary geometries, selected at -30 meter water depth (along stations C, D and E) of the Laohutan Bay, are perpendicular to the west, the south and the east (Figure 5). The three boundary conditions are determined using the harmonic analysis of the actual tide level: $z = z(x, y, t)$. The estimated friction Manning coefficient M of sea bed in the Bay is 22 m$^{1/3}$/s. The influence of the fluid viscosity is defined by eddy-viscosity coefficient E which can be obtained from the Smagorinsky equation (1963). Based on above mentioned parameters, Figures 6(a) ~ 6(c) show the typical results of tide level and current speed/direction at station A with field data. Good agreements were found between the field data and predicted data validate the model.

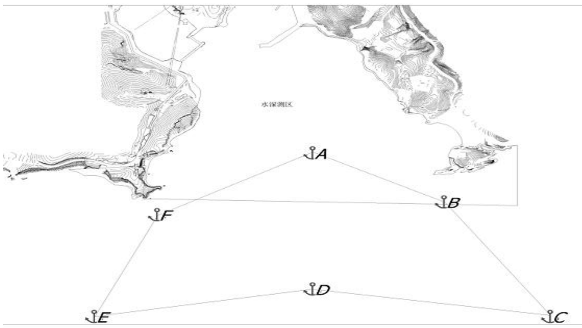

Figure 5: Locations of tidal stations

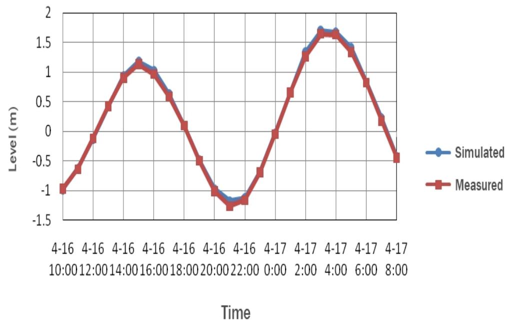

Figure 6(a): Comparison of tide level at point A

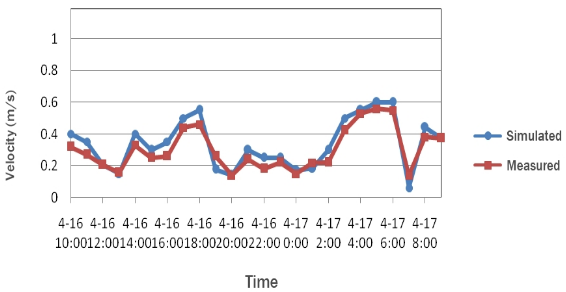

Figure 6(b): Comparison of current speed at point A

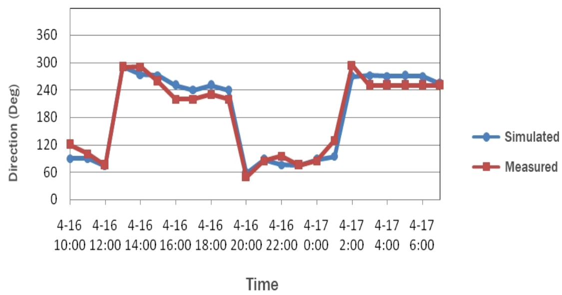

Figure 6(c): Comparison of current direction at point A

3. Scenario Studies

The Scenario studies of the flow field are defined as follows: (a) original topography (i.e., original coastal line, the submerged dyke and dam without gates); (b) scenario 1 (i.e., planned coastal line, the submerged dyke and dam with gates); and (c) scenario 2 which is the recommended scenario (i.e., planned coastal line, the submerged dyke with three openings and the dam with gates). The contour plots of original and planned topography are given in Figures 7 and 8.

Specifically, the lengths of submerged dyke and dam are 100 meter and 200 meter, respectively. The height of the dyke is 3.5 meter. In the scenario 2, each of the three openings on the submerged dyke is 10.0 meter in width and 3.5 meter in height with interval of 25 meter. The size of gate on the dam is approximated to 2.0 meter in width and 5.0 meter in height. The detail configuration of submerged dyke and dam is depicted in Figure 9.

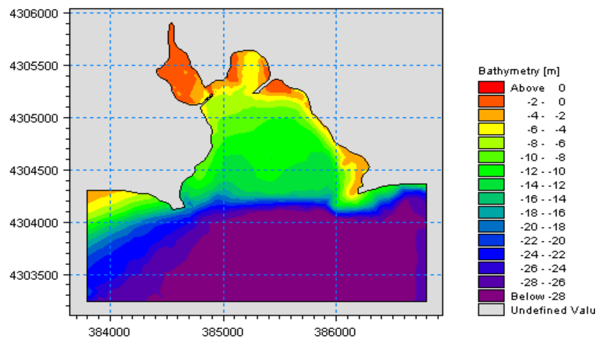

Figure 7: Original topography

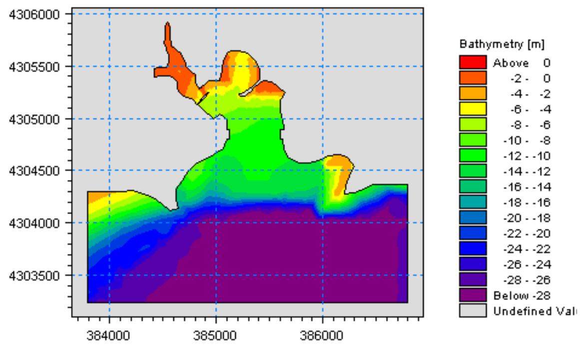

Figure 8: Planned topography

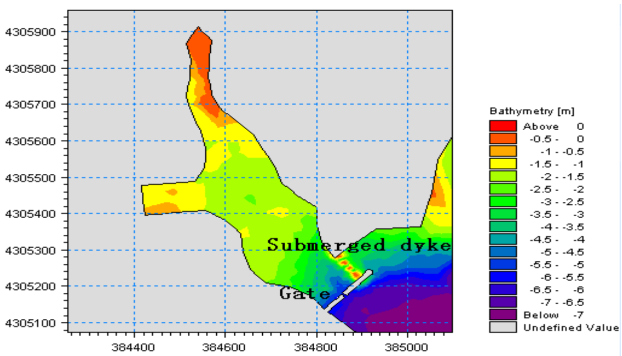

Figure 9: submerged dyke and the dam

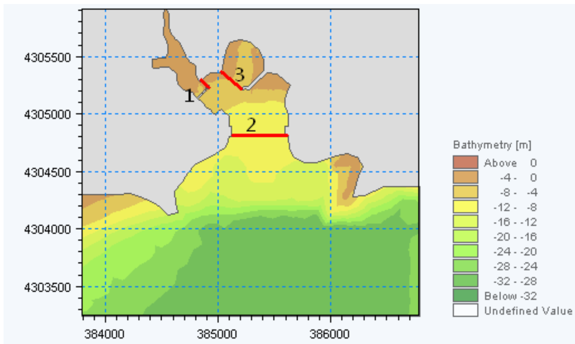

Figure 10: The defining cross-sections

Three cross-sections are defined to study the tidal influx and discharge: cross-section 1 for the entrance of submerged dyke; cross-section 2 for the entrance of the North Great Bridge; and cross-section 3 for the entrance of the wharf (Figure 10). To compare the current changes within the whole field, a set of control points are chosen at different positions of four zones (see Figure 11). Points K11 ~ K15 are in the zone1; points K33 ~ K39 are in the zone 2; point K30 is near the North Great Bridge; and points K31 and K32 are along the bathymetric line of -20 meter water depth (zone 4). The rest of the points are along the newly built coastal line.

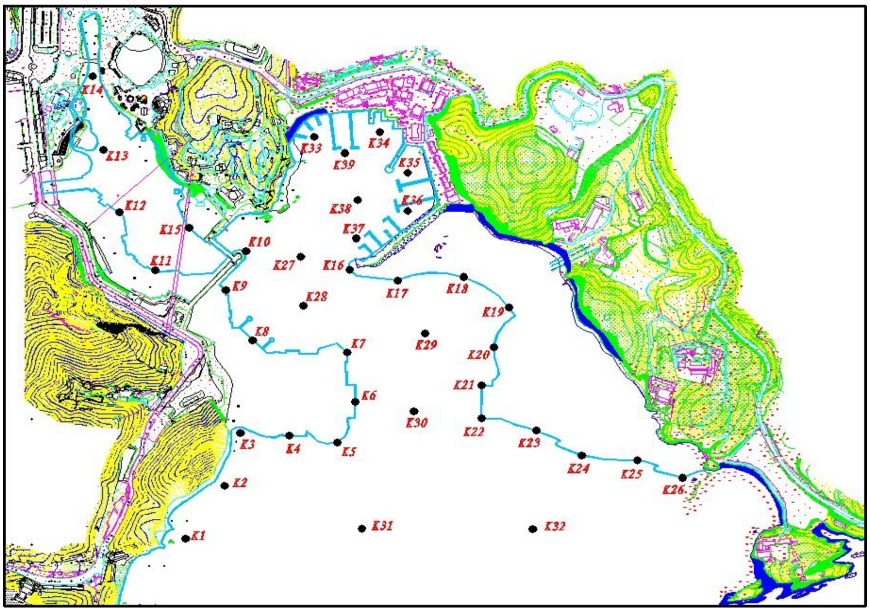

Figure 11: Distribution of control points for current

The simulations are executed for about 13 tidal cycles including high tides, middle tides and low tides; each tidal cycle is about 12.5 hours. The results of nearly one week time are sufficient to investigate the related problem.

4. The Analysis of the Flow Field

4.1 Comparison of flow field

Figures 12 and 13 are the contour plots of predicted velocity vector field of high tide at rising and falling time of Laohutan Bay under original topography. The figures show that at the open sea of the Laohutan Bay (-30 meter water depth), the tide flows from the east to the west at rising time or from the west to the east at falling time with an interval of half a tidal cycle (i.e., about 6 hours). The reciprocating flow along the coastal line forms a huge vortex among water depths -20 meter to -8 meter which rotates clockwise when the tide rises and anticlockwise when the tide falls. The contour plots also show that the velocity field of falling time is different from the rising time in the area of vortex.

Figures 14 and 15 are the contour plot of predicted velocity vector field of high tide at rising and falling time under planned topography for scenario 2. Compared to the large vortex resulted from the original topography at rising and falling time, the predicted vortex between -20 meter water depth and North Great Bridge is small in zone 4 and a new smaller vortex is created within the zone 3. This minor vortex will weaken the current running into the inner field of the bay (e.g., zone1 and zone 2). From the plots, it can also be seen that the velocity effecting scope of land reclamation can be confined to the area above -30 meter water depth.

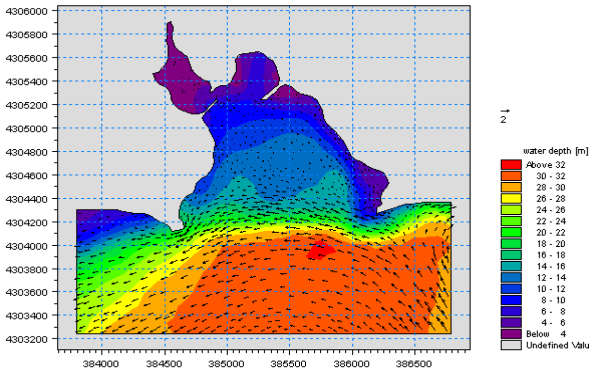

Figure 12: Predicted velocity field of high tide at rising time under original topography.

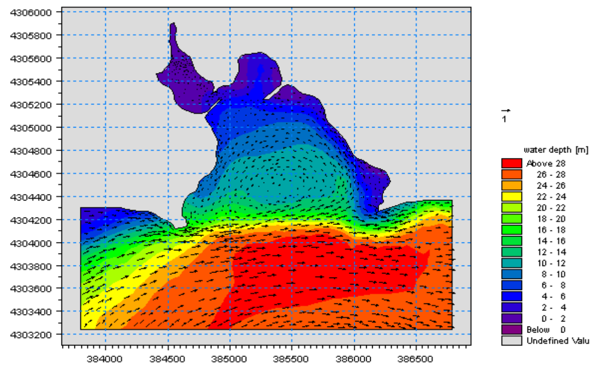

Figure 13: Predicted velocity field of high tide at falling time under original topography.

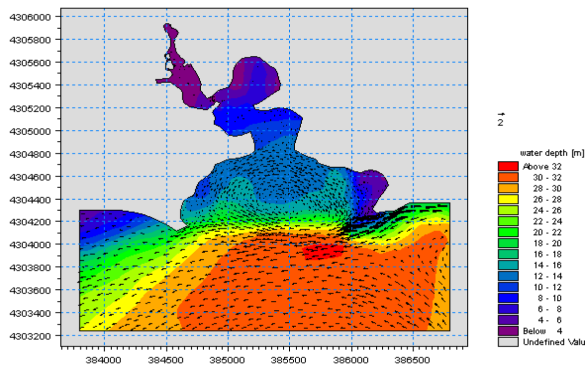

Figure 14: Predicted velocity field of high tide at rising time under planned topography

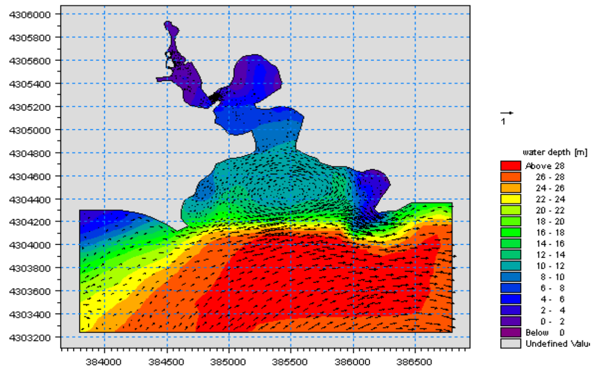

Figure 15: Predicted velocity field of high tide at falling time under planned topography

The quantitative comparisons of current speed/direction under original and planned topography are listed in Table 1 and Table 2. It can be observed that the similar tendency exists for both original and planned topography. In the zones 1 and 2, the current speed at rising time is faster than the one at falling time. In the zone 3, the two speeds are nearly the same. In the zone 4, the current speed at falling time is faster than the one at rising time. Under each topographic condition, the current speed in the zone 4 is the fastest. For instance, the maximum value of current speed at falling time at point K31 is 0.53m/s which is nearly 2.5 times of value at rising time under original topography. More important impact of reclamation is the current speed change at rising time. It can be found from table 2 that under planned topography the maximum value at rising time at point K32 is 0.67 m/s that is nearly 2.6 time of the value under original topography. This is partly due to the constriction of the cross-section 2.

Table 1: Current speed and direction under original topography

	Current speed(m/s)				Current direction (N degree)			
Points	Rising tide average	Rising tide max	Falling tide average	Falling tide max	Rising tide average	Rising tide max	Falling tide average	Falling tide max
K 10	0.05	0.15	0.03	0.05	268.57	312.18	71.20	84.81
K 11	0.04	0.14	0.01	0.02	156.82	271.11	129.04	103.76
K 13	0.07	0.13	0.03	0.03	152.77	150.83	162.38	162.57
K 14	0.03	0.03	0.01	0.02	50.29	352.01	171.10	170.68
K 27	0.04	0.06	0.06	0.07	259.90	298.65	73.81	83.69
K 28	0.07	0.10	0.09	0.11	223.80	255.57	56.08	63.15
K 29	0.12	0.20	0.15	0.19	221.67	270.88	92.21	95.03
K 30	0.16	0.24	0.11	0.13	207.65	256.54	68.13	78.75
K 31	0.14	0.23	0.47	0.53	152.43	173.77	273.51	273.62
K 32	0.21	0.26	0.35	0.40	52.72	23.16	283.51	283.82
K 38	0.02	0.03	0.01	0.01	75.28	71.00	133.34	136.45
K 39	0.01	0.02	0.00	0.01	279.30	322.64	59.51	91.69

Table 2: Current speed and direction under planned topography

	Current speed(m/s)				Current direction (N degree)			
Points	Rising tide average	Rising tide max	Falling tide average	Falling tide max	Rising tide average	Rising tide max	Falling tide average	Falling tide max
K 10	0.03	0.04	0.01	0.01	301.39	314.95	301.04	312.98
K 11	0.01	0.01	0.02	0.03	133.72	133.22	176.63	129.46
K 13	0.03	0.03	0.03	0.04	170.23	170.20	173.73	169.70
K 14	0.00	0.00	0.02	0.03	86.67	90.00	139.49	180.71
K 27	0.02	0.03	0.02	0.03	94.69	9.04	224.71	174.86
K 28	0.02	0.02	0.02	0.02	204.24	240.47	185.11	164.24
K 29	0.05	0.07	0.05	0.06	287.85	313.57	249.26	213.49
K 30	0.38	0.43	0.51	0.53	85.87	84.01	87.05	88.19
K 31	0.56	0.60	0.61	0.64	75.80	72.47	59.31	59.86
K 32	0.61	0.67	0.77	0.78	123.44	122.62	126.51	125.60
K 38	0.01	0.02	0.01	0.01	105.79	28.75	147.60	177.71
K 39	0.01	0.01	0.00	0.00	232.64	302.86	223.09	73.75

4.2 Influx and discharge analysis at different cross-sections

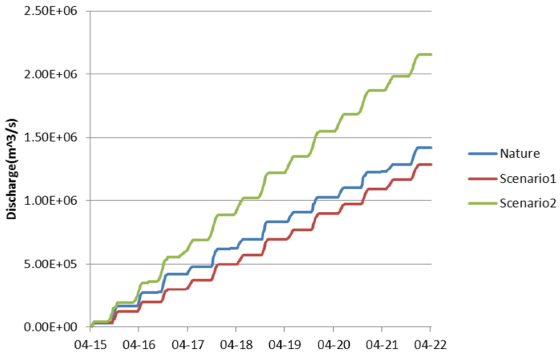

Figure 16: Influx of seven day tide cumulant on section 1

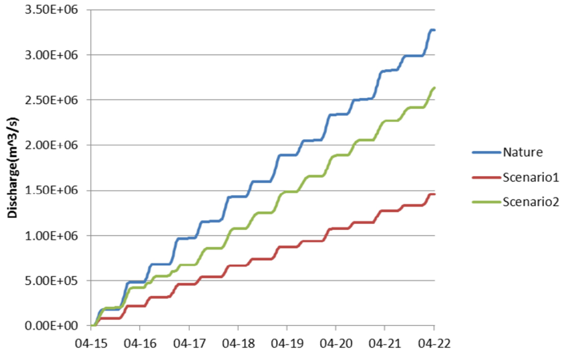

Figure 17: Discharge of seven day tide cumulant on section 1

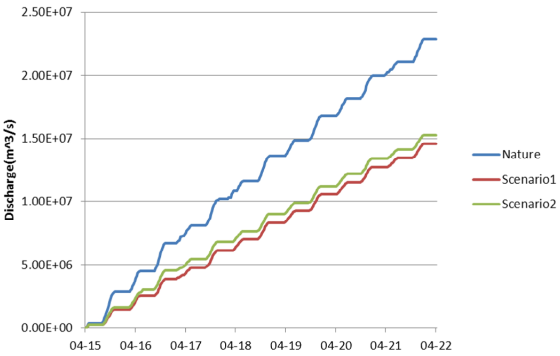

Figure 18: Influx of seven day tide cumulant on section 2

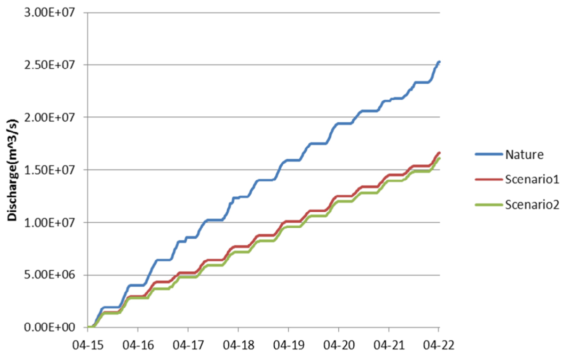

Figure 19: Discharge of seven day tide cumulant on section 2

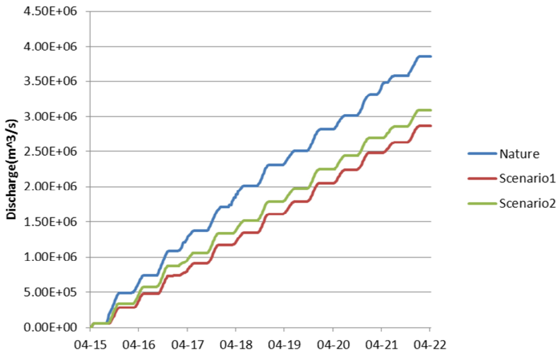

Figure 20: Influx of seven day tide cumulant on section 3

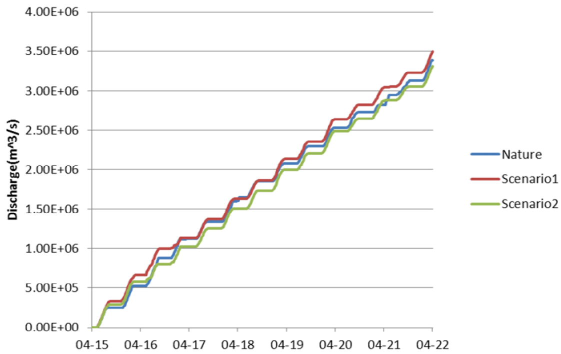

Figure 21: Discharge of seven day tide cumulant on section 3

The velocity analysis of current changes is not sufficient to provide a global evaluation of the influence of land reclamation, especially for the water exchange at the definite zones. The effects of different scenarios can be investigated comparing the results from the original topography of influx and discharge of tide accumulation at different cross-sections within seven day time with the simulation results (Figures 16~21). At very important cross-section 1, the influx and the discharge of scenario 1 are reduced by about 25 % and 50 %, respectively. While the influx of scenario 2 is increased by about 5 %, and the discharge is reduced only by about 15 % making the volume of influx larger than the volume of discharge. The increase of influx at cross-section 1 indicates the scenario 2 is effective solution. At the cross-section 2, the influx and discharge of scenario 1 and 2 are reduced by about 40 % while the difference of scenarios can be ignored. At the cross-section 3, the influxes of scenario 1 and 2 are reduced by about 25 % while the discharges of scenario 1 and 2 are nearly identical making the tidal level in zone 3 fall about 10 cm. Thus, the project basically meets the standards of environment protection.

5. Conclusion and Remarks

The following conclusions can be drawn from the present study:

（1） A hydrodynamic model was set up to investigate the current flow motion features within Dalian Laohutan Bay due to the land reclamation project. The tidal model is based on the numerical solution of the 2D depth averaged Reynolds averaged Navier-Stokes equations for incompressible flow. Finite volume method is used for spatial discretization, and adaptive time stepping technique is performed. A flexible triangle meshing scheme is adopted to meet the numerical precision for different zones in the numerical domain. A high-order k-ε turbulence closure model is used, and the Courant number (C) was controlled to be less than 0.8 to maintain the numerical stability.

（2） The validation of the model shows that the simulated tide level and the current speed/direction under original topography are in good agreement with the field measurements indicating that the study method and result are reliable and accurate.

（3） The validated model was used to assess the effect of the land acclamation project with various boundary conditions to reduce the impact on the water quality in the bay. A series of simulations for three scenarios were executed. With the analysis of flow field and the investigation of influx and discharge at different cross-sections, it can be concluded that the effecting scope of land reclamation is confined to the zones above -30 meter water depth. The results also show that the scenario 2 is suitable for water exchange within the inner field of the bay meeting the water quality requirement.

References

1. Li, S.S., Shi, Z. and Liu, Y.Z. 2001. 2DV FEM Numerical Model of Estuarine Tidal Flow. Marine Sciences, 25(9): 39-44. (in Chinese)
2. Zhang, C.Z., Yang, L.W. and Dou, Z.X. 1990. Finite Element Model of Shallow Water Circulation with Moving Tidal Boundary. ACTA OCEANOLOGICA SINICA, 12(1):1-13.(in Chinese)
3. Stansby, P.K. 1997. Semi-implicit Finite Volume Shallow-water Flow and Solute Transport Solver with k-ε Turbulence Model. Interactional Journal for Numerical Methods in Fluids, 125(3):285-313.
4. Cushnlan-Roisin, B. and Naimie, C.P.E. 2002. A 3D Finite-Element Model of the Adriatic tides. Journal of Marine Systems, (37): 279-297.
5. Ye, H.T., Wang, Y.G. and Cao, B. 2007. Tidal Prism of Sansha Bay and its Water Exchange with the Open Sea. Journal of Hohai University(Natural Sciences), 35(1):96-98.(in Chinese)
6. Han, K., Zhang, C.Z., Zhang, Y. and Yang, L.W. 1996. Numerical Study on Tidal Exchange in DALIAN Bay. Marine Science Bulletin, 15(2): 87-91.(in Chinese)

7. He, B.M. and Wei, M.X. 2004. The Characteristics of the Bionomical Environment in Qinzhou Bay and the Relationship Between the Characteristics and the Self-purifying Conditions of the Water Body. Marine Science Bulletin, 23(4): 50-54.(in Chinese)
8. MIKE 21. 2007. Tidal Analysis and Prediction Module Scientific Documentation, DHI WATER & ENVIRONMENT.
9. MIKE 21. 2007. FLOW MODEL FM Hydrodynamic and Transport Module Scientific Documentation, DHI WATER & ENVIRONMENT.
10. Smagorinsky, J. 1963. General Circulation Experiments with the Primitive Equations. Monthly Weather Review, 91(3): 99–164.